ChemCatChem

Research Article
doi.org/10.1002/cctc.202300418

Chemistry Europe
European Chemical
Societies Publishing

www.chemcatchem.org

Amino-Modified Polymer Immobilized Ionic Liquid Stabilized Ruthenium Nanoparticles: Efficient and Selective Catalysts for the Partial and Complete Reduction of Quinolines

Adhwa A. Alharbi,[a] Corinne Wills,[a] Thomas W. Chamberlain,*[b] Richard A. Bourne,[b] Anthony Griffiths,[b] Sean M. Collins,[b] Kejun Wu,[b] Pia Mueller,[b] Julian G. Knight,[a] and Simon Doherty*[a]

This article is dedicated to the memory of Professor Stephen A. Westcott, a great ambassador for chemistry in Canada and across the globe and the best and most sincere of friends.

RuNPs stabilised by amino-decorated imidazolium-based polymer immobilized ionic liquids catalyse the dimethylamine borane mediated reduction of quinolines to 1,2-dihydroquinoline (DHQ) and 1,2,3,4-tetrahydroquinoline (THQ). Partial reduction of 3-substituted quinolines to the corresponding 1,2-dihydroquinoline was achieved with 100% selectivity in toluene under mild conditions. This is the first report of the selective partial reduction of 3-substituted quinolines to the corresponding 1,2-dihydroquinolines with a heterogeneous nanoparticle-based catalyst. A wide range of substituted quinolines have also been reduced to the corresponding 1,2,3,4-tetrahydroquinoline with high selectivity and good yields by adjusting the reaction time. The 1,2-dihydroquinolines readily release dihydrogen in toluene at 60 °C in the absence of catalyst with no evidence for disproportionation and as such are potential organo-hydride reagents. The initial TOF of 610 mol quinoline converted mol Ru^{-1} h^{-1} for the reduction of quinoline is among the highest to be reported for a metal nanoparticle-based catalyst and the conversion of 96% obtained after 4 h at 65 °C is significantly higher than its platinum nanoparticle counterpart PtNP@NH$_2$-PEGPIILS as well as 5 wt/% Ru/C, which only reached 9% and 11% conversion, respectively, at the same time. Hot filtration experiments showed that the active species was heterogeneous.

Introduction

The tetrahydroquinoline motif is an important class of heterocycle as it is present in naturally occurring alkaloids with interesting biological activities (e.g. (−)-cuspareine, virantmycin, benzastatin, aflaquinolones and aspoquinolones), bioactive compounds with antiviral, antibacterial, antifungal and anticancer activity and agrochemicals with promising insecticidal, herbicidal, and fungicidal activities and has potential applications as a liquid organic hydrogen storage material.[1a–f] The selective reduction of quinoline is a particularly attractive approach for the synthesis of this motif as it is operationally straightforward compared with alternative multistep procedures involving metal catalysed intramolecular N–C and C–C bond forming cyclizations, cycloadditions and rearrangements.[1a–c] While homogeneous catalysts based on precious metals such as Rh, Ru, Pt, Pd and Ir have been developed,[1a,2a–h] such catalysts are costly and difficult to recover and reuse, the use of a stoichiometric amount of co-catalyst hinders its reuse and diminishes the green credentials and they are not suitable for integration into a continuous flow system. In contrast, supported metal nanoparticles appear to be far more versatile with several advantages as they can be recovered and reused in a simple filtration protocol, the catalyst is often compatible with sustainable and green solvents, the catalyst can be integrated into a continuous flow process for scale-up and catalyst efficiency can be modified by controlling the growth and size of the NPs.[3a–d] To this end, the selective reduction of quinoline to 1,2,3,4-tetrahydroquinoline has been catalysed by nanoparticle-support systems such as RuNPs/hydroxyapatite,[4] RuNPs/ionic liquids,[5] dendrimer stabilised MNP (M=Pd, Pt, Rh),[1f] polymer supported PdNPs,[6] PtNP/CeO$_2$,[7] RuNPs/N-doped carbon,[8] RhPt/oxide,[9] AuNP/SBA-15,[10] AuNPs supported on TiO$_2$,[11] PEG-stabilized RhNPs,[12] Ru isolated on nitrogen-doped

[a] A. A. Alharbi, Dr. C. Wills, Dr. J. G. Knight, Dr. S. Doherty
Newcastle University Centre for Catalysis (NUCAT)
School of Chemistry
Bedson Building
Newcastle University
Newcastle upon Tyne, NE1 7RU (UK)
E-mail: simon.doherty@ncl.ac.uk
Homepage: https://www.ncl.ac.uk/nes/people/profile/simondoherty.html

[b] Dr. T. W. Chamberlain, Prof. R. A. Bourne, A. Griffiths, Dr. S. M. Collins, Dr. K. Wu, Dr. P. Mueller
Institute of Process Research & Development School of Chemistry and School of Chemical and Process Engineering
University of Leeds
Woodhouse Lane, Leeds, LS2 9JT (UK)
E-mail: t.w.chamberlain@leeds.ac.uk
Homepage: https://eps.leeds.ac.uk/chemistry/staff/4213/dr-tom-chamberlain

ChemCatChem

Research Article
doi.org/10.1002/cctc.202300418

Chemistry Europe
European Chemical
Societies Publishing

porous carbon,[13] oxide supported RuNPs,[14] thermoregulated phase-transfer Pt nanocatalysts,[15] N-graphene-modified CoNPs,[16] AuPt@SBA-15,[17] Fe—N-doped carbon matrix,[18] and CoNPs in N-doped graphene.[19] While many of these systems exhibit high activity and good selectivity profiles, harsh conditions are sometimes required and the nitrogen atom of the reactant or product can coordinate to the surface of the NP and deactivate or poison the catalyst;[1f,4,5,6,11,20a–b] as such there is considerable interest in developing more active systems that are tolerant towards poisoning by heteroatom donors. While NPs are typically immobilized on a support to prevent aggregation under the conditions of catalysis there is now an increasing body of evidence that the activity and selectivity of nanoparticle-based catalysts for hydrogenations can be enhanced by incorporating organic modifiers onto the support to modulate their surface electronic structure and/or steric environment[21a–e] or by tuning metal-support interactions.[7,21f–l] To this end, there have been numerous reports that the stabilisation of NPs on supports modified with an amine donor improves their activity and selectivity for the hydrogenation of a range of substrates including α,β-unsaturated carbonyls,[22] aromatic compounds,[23] alkynes,[24] nitroarenes[25] and carbon dioxide[26] as well as for the dehydrogenation of formic acid;[27] in the majority of cases this has been attributed to either the high surface electron density, the ultra-small size of the nanoparticles, effective dispersion of the nanoparticles or a cooperative role in the elementary steps of the catalytic cycle. In particular, a significant enhancement in the turnover frequency for the selective hydrogenation of quinoline catalysed by palladium nanoparticles supported on amine rich silica hollow nanospheres when compared with their unmodified counterparts was attributed to the ultra-small particle size and high surface electron density resulting from coordination of the amine to the NP surface.[23a] Other relevant examples include markedly higher selectivity and activity for the semi-hydrogenation of alkynes to alkenes with palladium nanoparticles stabilised by an amino-polymer silica composite[24b] or an amine-modified silica surface;[24c] in both cases their unmodified counterparts were markedly less selective. High chemoselectivity for the hydrogenation of the C=O bond in cinnamaldehyde was obtained with platinum nanoclusters confined in the cavities of UiO-66-NH₂, whereas Pt nanoclusters supported on the external surface of the MOF and a commercial catalyst 5% Pt/C were much less selective.[22c,d] Similarly, monodisperse CoPt₃ nanoparticles capped with a long chain amine were markedly more selective catalysts for the hydrogenation of the C=O bond in cinnamaldehyde than their short chain counterparts.[22e]

We have recently been exploring the effect on catalyst performance of incorporating heteroatom donors into polymer immobilised ionic liquid (PIIL) supports for the stabilisation of nanoparticles, on the basis that the covalently grafted ionic liquid would stabilise the nanoparticles through weak electrostatic interactions to the surface in much the same manner as a conventional ionic liquid, while the heteroatom donor would supplement this stabilization and prevent aggregation under the conditions of catalysis by coordinating to the surface metal atoms.[28] To this end, our initial foray has demonstrated a beneficial effect as PdNPs supported on polyethylene glycol-

modified phosphine-decorated PIIL is a highly selective catalyst for the hydrogenation of α,β-unsaturated ketones in water,[28a] the aqueous phase reduction of nitroarenes[28] and the Suzuki-Miyaura cross coupling.[28c] Related studies include efficient and selective hydrogenation of aryl and heteroaryl ketones and levulinic acid,[28d] facile hydrolytic evolution of hydrogen from sodium borohydride[28e–f] and the partial selective reduction of nitroarenes to N-arylhydroxylamines and azoxyarenes[28g–h] using RuNPs and AuNPs stabilised by a phosphine oxide-decorated PIIL. The increasing number of reports of an enhancement in catalyst performance for nanoparticles stabilised by an amino-modified support has prompted us to extend this programme to explore the influence on catalyst efficacy of amine-decorated polymer immobilised ionic liquid supports by varying the density and type of amine donor. Herein, we report that RuNPs stabilised by an amine-decorated polymer immobilised ionic liquid catalyses the selective reduction of quinoline and its derivatives under mild conditions to afford the corresponding 1,2,3,4-tetrahydroquinolines in high yields with TOFs that are among the highest to be reported for the RuNP catalysed transfer hydrogenation of this class of substrate. This reduction was shown to occur stepwise via reversible formation of the 1,2-DHQ which was subsequently reduced to the 1,2,3,4-THQ (Scheme 1). Moreover, the transfer hydrogenation of 3-substituted quinolines occurred with complete selectivity for the partially reduced 1,2-dihydroquinolines, which are potentially versatile synthons to chiral tetrahydroquinolines[1] as well as reducing agents for use in transfer hydrogenations[29] or direct alkylation of anilines using alcohols via borrowing hydrogen.[30] This is the first example of a metal NP catalysed hydrogenation of quinoline using dimethylamine borane as the hydrogen source and although examples of metal-free and metal NP catalysed reductions of quinoline with amine borane have been reported, the TOFs are rather low, and a large excess of hydrogen donor is required.[31a–f]

Results and Discussion

Catalyst Synthesis and Characterisation

The amine decorated polymer immobilised ionic liquid stabilised RuNP catalyst required for this study was prepared by wet impregnation of the corresponding amine modified imidazolium based polystyrene (**1**)[28c,f] with ruthenium trichloride to afford a precursor with a ruthenium to amine ratio of one; this was then reduced *in situ* with an excess of NaBH₄ to afford RuNP@NH₂-
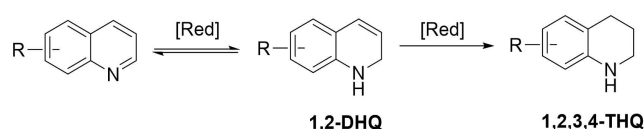
Scheme 1. RuNP–catalysed reduction of quinolines via reversible formation of the 1,2-DHQ and its subsequent reduction to the corresponding 1,2,3,4-THQ.

PEGPIILS (**2**), which was isolated in good yield as a fine free-flowing dark brown powder after work-up (Figure 1). The catalyst was characterised by a combination of solid-state NMR spectroscopy, IR spectroscopy, SEM, TEM, EDX, and XPS and the ruthenium loading was determined to be 0.69 mmol g^{-1} using ICP-OES. The solid state ^{13}C NMR spectrum of **2** contains a distinctive set of resonances between δ 123 and 147 ppm which correspond to the aromatic carbon atoms of the styrene as well as the C(2) and C(3,4) carbon atoms of the imidazolium ring, signals between δ 11 and 51 ppm belong to the methylene and methine carbon atoms of the polystyrene backbone and the methyl group attached to the imidazolium ring and resonances at δ 70 and 58 ppm belong to the methylene carbon atoms of the polyether chain and its terminal OMe, respectively.
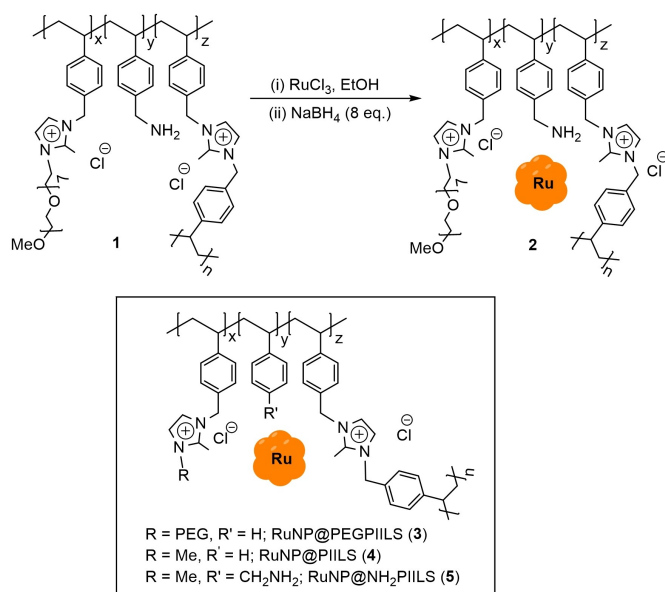
The surface of catalyst **2** was characterised by X-ray photoelectron spectroscopy (XPS) by analysing the Ru 3p region. This was analysed because of overlap of the C 1s and Ru 3d regions (Figure 2). The Ru 3p$_{3/2}$ and 3p$_{1/2}$ peaks for **2** appeared at 463.2 eV and 485.3 eV, respectively, which appear at higher binding energies compared to those reported for metallic Ru(0) (461.3 eV and 483.5 eV)[32] and are consistent with RuO$_2$ which has reported binding energies of 463.0 eV and 485.2 eV.[32] The presence of RuO$_2$ species most likely results from a degree of surface oxidation of the preformed metallic Ru nanoparticles. TEM micrographs of **2** revealed that the ruthenium nanoparticles were ultrafine and near monodisperse with an average diameter of 1.8±0.5 nm (Figure 3a-b) and EDX elemental mapping image (Figure 3b) revealed an even distribution and good dispersity of the RuNPs within the support, similar in structure to previously reported RuNP@PIILS catalysts.[28d] SEM images revealed that the catalyst material was far more granular than its polymeric counterpart, which appeared largely smooth.

Partial Reduction of Quinolines to 1,2-Dihydroquinoline and 1,2,3,4-Tetrahydroquinoline

The reduction of quinoline to 1,2,3,4-tetrahydroquinoline was identified as an ideal transformation to explore the efficiency of RuNP@NH$_2$-PEGPIILS as the tetrahydroquinoline motif is found in a wide range of bioactive compounds and agrochemicals; in addition, ruthenium nanoparticles are well-documented to be efficient catalysts for reductions. To this end, the sodium borohydride-mediated reduction of quinolines catalysed by hectorite-intercalated RuNPs was identified as a suitable benchmark comparison to assess its efficiency.[33a] A series of reactions were initially conducted to explore the effect of temperature, time, the amount and type of reducing agent, and the solvent on the conversion and selectivity, full details of which are presented in Table 1. Using recent literature protocols as a lead,[6b,33a,31b–d] a preliminary reaction conducted in water under nitrogen at 40 °C with a 0.1 mol% loading of catalyst and 2.5
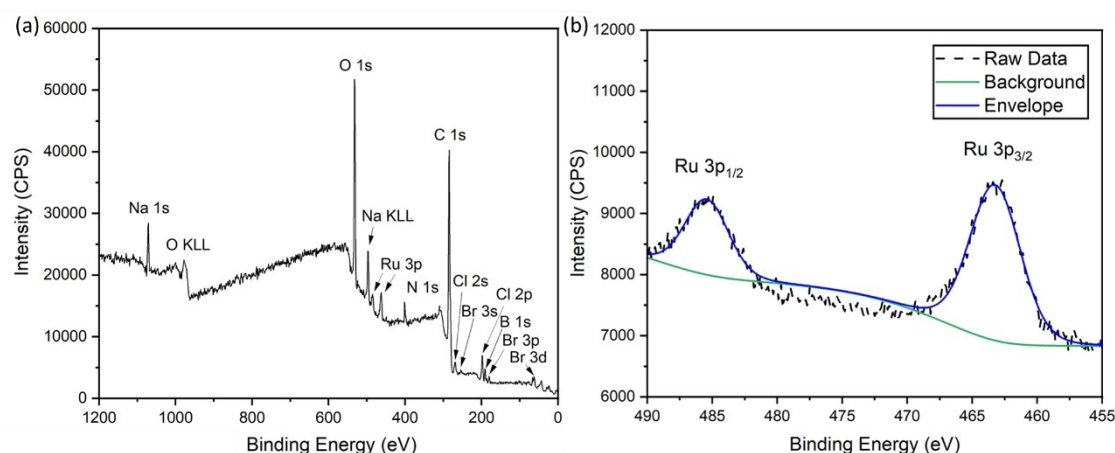

Figure 1. Synthesis of amino-decorated PIIL-stabilised ruthenium nanoparticles RuNP@NH$_2$-PEGPIILS (**2**) and composition of the PIIL-stabilised ruthenium nanoparticles **3–5**.

Figure 2. XPS data showing (a) the overall survey scan and (b) the Ru 3p$_{3/2}$ region of PIIL-stabilised ruthenium nanoparticles **2**.

ChemCatChem

Research Article
doi.org/10.1002/cctc.202300418

**Chemistry
Europe**
European Chemical
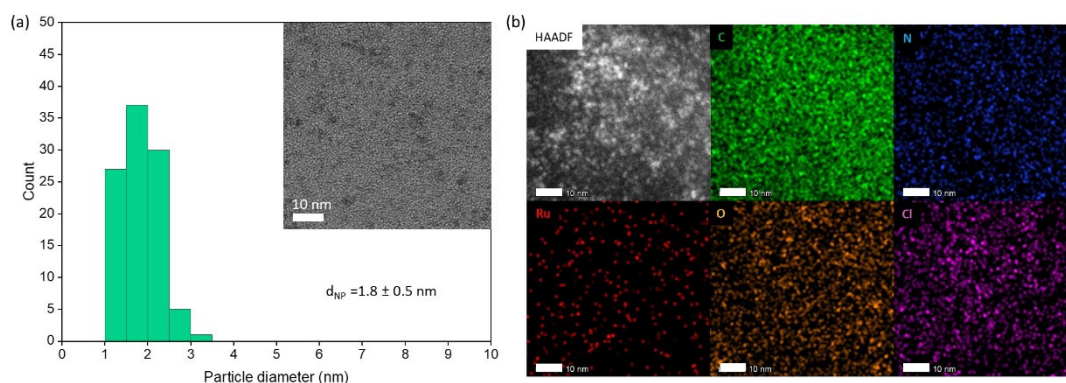Societies Publishing

Figure 3. (a) Size distribution of NPs in **2** determined by counting > 100 particles with HRTEM image inset and (b) HAADF image and EDX mapping of **2**. All scale bars are 10 nm (white).

Table 1. Selective reduction of quinoline to 1,2,3,4-tetrahydroquinoline as a function of catalyst, solvent, temperature, time, and hydride source.[a]

Entry	Catalyst [mol %]	Hydride [equiv.]	Temp [°C]	solvent	Conv. [%][b]	Selectivity [%][c]
1	**2** (0.1)	$NaBH_4$ (2.5)	40	H_2O	47	100
2	**2** (0.1)	$NaBH_4$ (5)	40	H_2O	54	100
3	**2** (0.1)	N_2H_4 (3)	40	H_2O	3	100
4	**2** (0.1)	$Me_2NH.BH_3$ (5)	40	H_2O	61	100
5	**2** (0.1)	$NH_3.BH_3$ (5)	40	H_2O	19	100
6	**2** (0.1)	$HCO_2H.NEt_3$ (5)	40	H_2O	0	–
7	**2** (0.1)	$Me_2NH.BH_3$ (5)	40	EtOH	24	100
8	**2** (0.1)	$Me_2NH.BH_3$ (5)	40	MeOH	31	100
9	**2** (0.1)	$Me_2NH.BH_3$ (5)	40	toluene	68	63[d]
10	**2** (0.1)	$Me_2NH.BH_3$ (5)	40	THF	24	100
11	**2** (0.1)	$NaBH_4$ (5)	40	toluene	3	100
12	**2** (0.1)	$NH_3.BH_3$ (5)	40	toluene	6	50
13	**2** (0.1)	$Me_2NH.BH_3$ (5)	50	toluene	72	79
14	**2** (0.1)	$Me_2NH.BH_3$ (5)	65	toluene	82	84
15	**2** (0.25)	$Me_2NH.BH_3$ (5)	65	toluene	96	99
16	**2** (0.5)	$Me_2NH.BH_3$ (5)	65	toluene	97	99
17	**2** (0.05)	$Me_2NH.BH_3$ (5)	65	toluene	61	54
18	**2** (0.25)	$Me_2NH.BH_3$ (2.5)	65	toluene	68	79
19	**2** (0.25)	$Me_2NH.BH_3$ (10)	65	toluene	98	99
20	**3** (0.25)	$Me_2NH.BH_3$ (5)	65	toluene	65	86
21	**4** (0.25)	$Me_2NH.BH_3$ (5)	65	toluene	43	75
22	**5** (0.25)	$Me_2NH.BH_3$ (5)	65	toluene	71	89
23	Ru/C (0.25)	$Me_2NH.BH_3$ (5)	65	toluene	11	100
24	PtNP (0.25)	$Me_2NH.BH_3$ (5)	65	toluene	13	100
25	**2** (0.25)	H_2 (1 atm)	65	toluene	14	100

[a] Reaction conditions: Conducted under a nitrogen atmosphere, 1 mmol quinoline, × mol% catalyst, 3 mL solvent, hydride source, 4 h, temperature, [b] % Conversion determined by ^1H NMR spectroscopy using dioxane as internal standard. Average of at least three runs, [c] Selectivity for 1,2,3,4-tetrahydroquinoline = [% 1,2,3,4-tetrahydroquinoline/(% 1,2,3,4-tetrahydroquinoline + % 1,2-dihydroquinoline)] × 100 %, [d] Selectivity for 1,2-dihydroquinoline.

mole equivalents of $NaBH_4$ gave 47% conversion to 1,2,3,4-tetrahydroquinoline as the sole product; this conversion only increased to 54% with 5 mole equivalents of $NaBH_4$ (Table 1, entries 1–2). Variation of the hydrogen donor under otherwise identical conditions revealed that the conversion improved to 61% with dimethylamine borane to afford 1,2,3,4-tetrahydroquinoline in 100% selectivity, while reductions with ammonia borane, hydrazine hydrate and formic acid triethylamine azeotrope gave either low or negligible conversions (Table 1, entries 3–6); as such, dimethylamine borane was identified as the hydrogen donor of choice for further optimisation studies. As the activity and selectivity profile of a heterogeneous catalyst is often sensitive to the solvent,[33a–c] a survey of the conversion and selectivity as a function of the solvent for the dimethylamine borane-mediated reduction of quinoline was undertaken at 40 °C using 0.1 mol% **2**. Under these conditions,

ChemCatChem

Research Article
doi.org/10.1002/cctc.202300418

Chemistry Europe
European Chemical
Societies Publishing

reactions conducted in methanol and ethanol resulted in slightly lower conversions of 31% and 24%, respectively, than in water which reached 61% conversion (Table 1, entries 7–8). The use of toluene as the solvent resulted in a slight increase in conversion to 68% but with a dramatic change in the selectivity profile to afford 1,2-dihydroquinoline as the major product (43%) together with 1,2,3,4-tetrahydroquinoline (25%); the identity of the former was confirmed by comparison of its characteristic ^{1}H NMR resonances with those of an authentic sample. Such a dramatic solvent dependent selectivity was surprising as reactions conducted in water, ethanol and methanol all gave 1,2,3,4-tetrahydroquinoline as the sole product, regardless of the conversion. The marked difference in selectivity between reactions conducted in water or a protic solvent compared with toluene may well be associated with the different pathways for hydrogen liberation as reactions in protic solvent involve hydrolysis and release three mole equivalents of hydrogen while reactions in toluene involve catalytic dehydrogenation and only liberate one equivalent. To this end, a reduction conducted under biphasic conditions in a 1:1 mixture of toluene and water only reached 16% conversion after 4 h, with 100% selectivity for 1,2,3,4-tetrahydroquinoline. Although THF has been reported to be the solvent of choice for the NP-catalysed reduction of quinoline,[34a–b] a reduction using 0.1 mol% **2 a** only reached 24% conversion after 4 h, with complete selectivity for 1,2,3,4-tetrahydroquinoline (Table 1, entry 10). A reduction was also conducted in toluene with 5 mole equivalents of sodium borohydride to assess the efficiency of this donor against dimethylamine borane in this solvent. Under otherwise identical conditions the conversion only reached 3% compared with 54% in water, which is most likely due to mass transfer limited reduction associated with the low solubility of sodium borohydride in toluene (Table 1, entry 11). Similarly, ammonia borane was also a poor hydrogen donor in toluene as a reduction of quinoline only reached 6% conversion to a mixture of 1,2-dihydroquinoline and 1,2,3,4-tetrahydroquinoline (Table 1, entry 12). Analysis of the reaction mixture revealed that the low conversion was probably due to formation of the quinoline-borane adduct, as evidenced by a characteristic signal at δ −13.8 ppm in the ^{11}B NMR ($^1J_{\text{B-H}} = 96$ Hz) spectrum and an additional set of resonances in the ^{1}H NMR spectrum consistent with those reported in the literature.[35]

Using toluene as the solvent and dimethylamine borane as the donor of choice, the conversion increased from 68% at 40°C to 72% at 50°C and ultimately to 82% with 84% selectivity for 1,2,3,4-tetrahydroquinoline when the reaction temperature was raised to 65°C (Table 1, entry 13–14). As near complete conversion with high selectivity for 1,2,3,4-tetrahydroquinoline could be obtained by extending the reaction time accordingly this temperature was used for further optimisation studies and to explore the range of substrates (see later). An increase in the catalyst loading to 0.25 mol% resulted in an increase in the conversion to 96% with 99% selectivity for 1,2,3,4-tetrahydroquinoline after 4 h at 65°C, while a further increase in the catalyst loading to 0.5 mol% only improved the conversion to 97% under the same conditions (Table 1, entries 15–16), indicating that the

reaction is mass transfer limited under these conditions. The efficacy of **2** was further tested by reducing the catalyst loading to 0.05 mol% which resulted in a concomitant reduction in the conversion to 61% with 54% selectivity for 1,2,3,4-tetrahydroquinoline after 4 h (Table 1, entry 17). As a large excess of reducing agent is often required for efficient transfer hydrogenation, the conversion was investigated as a function of the mole ratio of dimethylamine borane to quinoline. The conversion decreased quite dramatically from 94% with five equivalents of dimethylamine borane to 68% with 2.5 equivalents while an increase to 10 improved the conversion to 97% with 99% selectivity for 1,2,3,4-tetrahydroquinoline (Table 1, entries 18–19). A control reaction for the reduction of quinoline conducted in toluene in the absence of catalyst but with five equivalents of dimethylamine borane gave no conversion after 4 h, which confirmed the active role of the catalyst.

The influence on catalyst performance of the composition of the polymer, namely the amine and PEG components was explored by comparing the performance of catalysts with different modifications *i.e.* the amine free systems RuNP@PEG-PIILS (**3**) and RuNP@PIILS (**4**) as well as RuNP@NH₂-PIILS (**5**) which lacks the hydrophilic PEG chain (Scheme 1).[28f] The corresponding data in Table 1 (entries 20–22) reveals that removal of the surface grafted amine has a dramatic effect on the conversion as a reduction catalysed by 0.25 mol% RuNP@PEGPIILS (**3**) only reached 65% conversion with 86% selectivity for 1,2,3,4-tetrahydroquinoline after 4 h, compared with 96% conversion and 99% selectivity for **2**. Moreover, the use of RuNP@PIILS (**4**) as the catalyst under the same conditions resulted in a more significant drop in conversion to 43% *i.e.* both the PEG and the amino group appear to be required to achieve optimum efficiency. Finally, the conversion of 71%, with 89% selectivity for THQ, obtained with RuNP@NH₂-PIILS (**5**) is a marked improvement on the 43% conversion obtained with RuNP@PIILS (**4**), which may be taken as a measure of the influence of the amine on catalyst performance. While these modifications have demonstrated that each component has a direct and dramatic effect on the efficacy of the catalyst, further studies will be required to develop a full understanding of the precise role of the PEG and the amine *i.e.* whether the enhancement in performance for RuNPs supported on PEG-amine modified polymer is due to strong metal molecular support interactions (SMSSI), as previously reported by Yadav *et al.*,[27c,36] NP size, distribution and dispersion,[26b–c,27b,c,g,h,i] the balance of hydrophilicity/hydrophobicity and thereby access to the active site,[21a,27b,k] the surface electronic structure,[27a–c,f] or a cooperative role of the amine in the elementary steps of the catalytic cycle.[26a–c,27l]

The efficiency of **2** as a catalyst for the reduction of quinoline was also compared against that of commercially available Ru/C (5 wt%) and under the same conditions only reached 11% conversion, albeit with 100% selectivity for 1,2,3,4-tetrahydroquinoline after 4 h (Table 1, entry 23). As there have been several reports of efficient and selective hydrogenation or reduction of quinoline catalysed by PtNP-based systems including PtNPs stabilized by G4OH PAMAM dendrimers supported in SBA-15,[1f] PtNPs stabilized by bulky terphenylphosphines[31b] and PtNPs

ChemCatChem

Research Article
doi.org/10.1002/cctc.202300418

Chemistry
Europe
European Chemical
Societies Publishing

anchored on jute plant stems,[37] the efficacy of **2a** was compared against its platinum counterpart PtNP@NH$_2$-PEGPIILS. Surprisingly, under the optimum conditions described above, the dimethylamine borane-mediated reduction of quinoline catalysed by 0.25 mol% PtNP@NH$_2$-PEGPIILS only reached 13% conversion after 4 h whereas **2** reached 96% at the same time (Table 1, entry 24). While such a poor conversion was unexpected, a study of the hydrolytic evolution of hydrogen from NMe$_2$H.BH$_3$ using 0.1 mol% **2** and PtNP@NH$_2$-PEGPIILS revealed that the former is a markedly more efficient catalyst as it achieves near quantitative liberation of hydrogen after only 28 min with an initial TOF of 3,100 h^{-1}, while its platinum counterpart PtNP@NH$_2$-PEGPIILS only liberated 11% hydrogen at the same time with an initial TOF of 320 h^{-1} (Figure 4a). Similarly, **2** is also a more efficient catalyst for the corresponding dehydrocoupling of NMe$_2$H.BH$_3$ in toluene than its platinum counterpart (Figure 4b), although qualitatively the difference is not as marked as the hydrolysis. Thus, the poor conversion obtained for the reduction of quinoline using PtNP@NH$_2$-PEGPIILS as the catalyst may well be associated with the low availability of hydride species at the NP surface resulting from the slow transfer/release of hydrogen from the dimethylamine borane adduct. In order to investigate whether the dimethylamine borane mediated reduction occurred with molecular hydrogen liberated from the donor

or directly involving a borane-derived surface hydride species, a catalytic reduction was conducted under 1 atmosphere of hydrogen reasoning that a high conversion would be expected if the reduction involved molecular hydrogen. However, under otherwise identical conditions, the conversion only reached 14% with 100% selectivity for 1,2,3,4-tetrahydroquinoline (Table 1, entry 25); this is markedly lower than the 96% conversion obtained with dimethylamine borane and indicates that the reduction most likely occurs via a heterolytic pathway involving a surface mediated hydride transfer rather than activation of molecular hydrogen released from the surface (see later).

Having identified conditions to obtain high conversion and selectivity for 1,2,3,4-tetrahydroquinoline, the composition was monitored as a function of time in d$_8$-toluene at 65 °C to explore the reaction profile and obtain an initial TOF to compare its efficacy against previously reported systems. A series of parallel reactions were conducted across a range of times and the composition quantified by ^{1}H NMR spectroscopy. The resulting composition-time profile in Figure 5 shows rapid consumption of quinoline with concomitant formation of 1,2,3,4-tetrahydroquinoline in the early stages of the reaction (15 min) and a gradual build-up of 1,2-dihydroquinoline to 17% over the first 2 h, which was gradually consumed at longer reaction times to afford 1,2,3,4-tetrahydroquinoline as the sole product after 10 h. A similar profile was obtained with a catalyst loading of 0.25 mol%, although the maximum concentration of 1,2-dihydroquinoline only reached 6% and complete conversion to 1,2,3,4-tetrahydroquinoline was achieved after *ca.* 4 h (Figure S1 in the supporting information). These profiles are consistent with facile reduction of the 1,2-dihydroquinoline generated in the early stages of the reaction and explains the low selectivity for the partial reduction of quinoline. A comparison of the efficacy of **2** as a catalyst for the transfer hydrogenation of quinoline to 1,2,3,4-tetrahydroquinoline against other nanoparticle-based systems revealed that **2** is among the most active to be reported. For example, the initial TOF of 610 mole quinoline converted mol Ru^{-1} h^{-1} obtained at 65 °C is substantially higher than the 12 mole product mol Ru^{-1} h^{-1} obtained at

Figure 4. Volume of hydrogen generated against time for the release of hydrogen from a 0.28 M aqueous solution of NMe$_2$H.BH$_3$ as a function of time at 303 K catalysed by 0.1 mol% RuNP@NH$_2$-PEGPIILS (blue) and 0.1 mol% PtNP@NH$_2$-PEGPIILS (red) (a) hydrolytic evolution conducted in water (b) dehydrocoupling conducted in toluene. Each volume is an average of three runs.
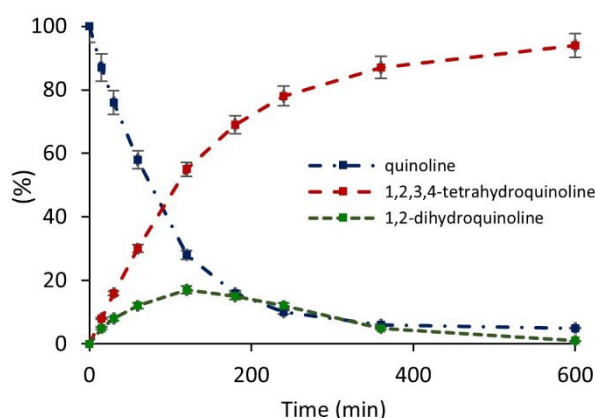

Figure 5. Reaction composition as a function of time for the dimethylamine borane-mediated reduction of quinoline in toluene at 65 °C catalysed by 0.1 mol% **2**.

ChemCatChem

Research Article
doi.org/10.1002/cctc.202300418

Chemistry Europe
European Chemical
Societies Publishing

60 °C with RuNPs intercalated in hectorite,[33a] 13 mole product mol Pd^{-1} h^{-1} obtained with PdNPs stabilised in a ethyl methacrylate and ethylene glycol dimethacrylate based co-polymer,[6b] 51 mole product mol Au^{-1} h^{-1} for AuNP supported on amino-modified SAB-15,[38] 2 mole product mol Pt^{-1} h^{-1} for phosphine-decorated platinum nanoparticles,[31b] Ni dispersed in porous carbon NiNPs@PC (TOF of 310 mole product mol Ni^{-1} h^{-1} in water/alcohol at room temperature)[31d] and even comparable to that of 600 mole product mol Au^{-1} h^{-1} obtained at 130 °C with AuNP supported on rutile.[39] As there are relatively few reports of the transfer hydrogenation of quinoline to tetrahydroquinoline catalysed by nanoparticle-based systems the comparison was extended to include nanoparticle catalysed hydrogenations. Gratifyingly, the TOF obtained with **2** is also comparable to or higher than the majority of these systems including RuNPs dispersed in 3D-interconnected hierarchical porous N-doped carbon (TOF of 654 h^{-1} in EtOH at 100 °C),[40] a well-dispersed core shell nanocatalyst, Ru-SiO$_2$@mSiO$_2$ (TOF of 30 h^{-1} in water at 90 °C),[33c] thermoregulated phase-transfer Pt nanoparticles (TOF of 193 h^{-1} in water at 80 °C),[15] RuNPs stabilised by a diol functionalised ionic liquid (TOF of 10 h^{-1} in [BMMIM]NTf$_2$ at 80 °C),[5] polymer supported PdNPs (TOF of 22 h^{-1} in MeOH/water at 80 °C),[6a,b] phosphine-functionalised ionic liquid-stabilised rhodium and ruthenium NPs (TOF of 20 h^{-1} in [BMIM][PF$_6$] at 50 °C and 71 h^{-1} in water at 50 °C, respectively)[33b,41] and RuNPs supported on biomass-derived N-doped porous 2D-carbon nanosheets (TOF of 96 h^{-1} in ethanol at 40 °C).[42] Other relevant comparisons include PdNPs sup-ported on amine-rich hollow silica nanospheres (TOF of 135 h^{-1} in cyclohexane at 50 °C),[23a] ionic liquid stabilised NiNPs (TOF of 29 h^{-1} in EtOH at 75 °C),[43] NHC-stabilised RhNPs (TOF of 496 h^{-1} in THF at 60 °C),[34b] PEG-stabilized RhNPs (TOF of 182 h^{-1} in toluene at 80 °C),[12] 12CaO·7Al$_2$O$_3$ loaded with RuNPs (TOF 52 h^{-1} at 80 °C),[14] AuNPs and AuPt bimetallic nanoalloy nano-particles confined in SBA-15 (TOF of 20 h^{-1} in water at 100 °C and 34 h^{-1} in water at 25 °C),[10,17] PtRuNi/C (TOF of 329 h^{-1} in toluene at 100 °C),[44] Ru clusters confined in hydrogen-bonded organic frameworks (TOF of 3 h^{-1} in water at 80 °C),[45] PdNPs stabilised by carbon-metal covalent bonds (TOF of 6 h^{-1} in water at room temperature),[46] AuNPs supported on TiO$_2$ (TOF of 29 h^{-1} in toluene at 60 °C),[11] bimetallic CoRhNPs immobilised on an imidazolium-based ionic liquid phase (TOF of 4 h^{-1} at 150 °C),[47] a RhNPs-Lewis acid ionic liquid catalyst (TOF of 6 h^{-1} in [BIMIM][BF$_4$] at 80 °C),[48] PdRu@PVP (TOF of 2 h^{-1}, solventless at 25 °C),[49] Ru nanoclusters supported on Ti$_3$C$_2$T$_x$ nanosheets (TOF of 21 h^{-1} in ethanol/water at 55 °C),[50] RuNPs supported on nitrogen doped carbon (TOF of 20 h^{-1} in ethanol at 30 °C),[51] and isolated single ruthenium atoms anchored on the amine modified MOF UiO-66-NH$_2$ (TOF of 25 h^{-1} in THF at 100 °C).[52] While a significantly higher TOF of 3,400 h^{-1} has been obtained for the hydrogenation of quinoline using RuNPs immobilised on magnesium oxide as the catalyst, reactions were conducted at 150 °C under 50 atm of hydrogen.[34a]

The heterogeneous nature of **2** was explored by conducting a hot filtration experiment which involved running two reactions in parallel using 0.1 mol% **2** with five mole equivalents of dimethylamine borane to catalyse the reduction of quinoline.

When the conversion reached *ca.* 40 % one of the reaction mixtures was filtered through a 45-micron syringe filter and the composition of the resulting filtrate monitored as a function of time for a further 120 min. The conversion-time profile for the second reaction was used as a benchmark. The corresponding composition-time profile (Figure 6) clearly shows that filtration quenches the reduction which suggests that the active species has been removed *i.e.*, the catalyst is either heterogeneous and has been removed or leaching of ruthenium generates a less or inactive species. Minor changes in the composition of the reaction mixture after the hot filtration can be attributed to the release of hydrogen from the 1,2-dihydroquinoline to generate quinoline as this partial reduction has been shown to be reversible (see later). Analysis of the organic filtrate collected after the filtration revealed that the ruthenium content was below the detection limit of the ICP-OES suggesting that the catalyst is most likely heterogeneous, and that leaching is not significant. In a complimentary hot filtration experiment, a reduction was allowed to reach complete conversion after which the solution was filtered through a 45-micron syringe filter, a fresh portion of quinoline added to the filtrate and the composition monitored for a further 4 h. There was no further measurable conversion of quinoline, even after stirring for a further 4 h at 65 °C, which provides additional support that the filtration removed the active species.

The stability and longevity of **2** as a catalyst for the dimethylamine borane-mediated transfer hydrogenation of quinoline was investigated by monitoring the performance profile during reuse to assess its suitability for integration into a continuous flow system, as previously described for the sodium borohydride-mediated reduction of nitrobenzene using PdNP@PPh$_2$-PEGPIILS as the catalyst.[28b] The practical difficulty associated with recovering a small amount of catalyst by filtration meant that it was not possible to conduct a conven-tional recycle experiment. Instead, the conversion and selectiv-ity profile for the dimethylamine borane-mediated reduction of
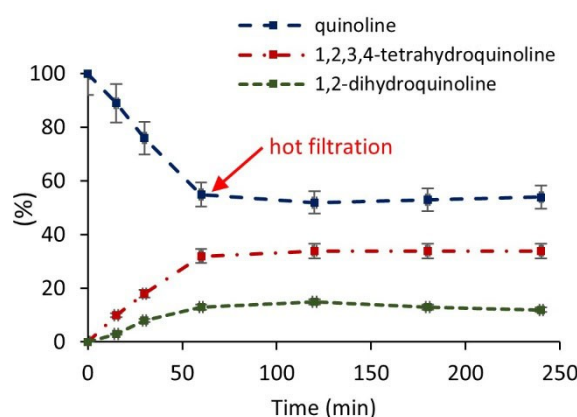

Figure 6. Hot filtration experiment for the dimethylamine borane-mediated transfer hydrogenation of quinoline in toluene at 65 °C catalysed by 0.1 mol% **2** showing that the reduction is completely quenched after filtration at t = 60 min. Red line – composition of quinoline, blue line – composition of 1,2,3,4-tetrahydroquinoline and green line – composition of 1,2-dihydroquinoline.

ChemCatChem

Research Article
doi.org/10.1002/cctc.202300418

Chemistry
Europe
European Chemical
Societies Publishing

quinoline was monitored as a function of time after which additional portions of quinoline and dimethylamine borane were added without work-up or catalyst treatment. The composition of the resulting mixture was then monitored again as a function of time for a further 4 h and the protocol repeated for three additional cycles to determine the efficiency of **2** as a function of the reaction time and reuse number. The data in Figure 7 shows that the catalyst retains high selectivity in each run and that there is a gradual decrease in conversion, which is most evident in the fourth run, however, the conversions could be improved by extending the reaction time to 8 h. Such a decrease in conversion with reuse may be due either to leaching of ruthenium to generate soluble homogeneous species that are less active, which would reduce the size and modify the morphology and hence efficacy of the resulting NPs, aggregation to form larger less efficient nanoparticles or deactivation/passivation of the catalyst by saturation of the surface-active ruthenium sites by the nitrogen donor in the tetrahydroquinoline product. Analysis of the organic phase collected after the fourth reuse revealed that the ruthenium content was below the detection limit of the ICP-OES indicating that the drop in conversion is unlikely to be due to leaching of the catalyst to generate a homogeneous species that was less active, however, analysis of the ruthenium content in this manner does not distinguish a pathway that involves leaching and re-deposition. A TEM of the organic phase remaining after the 4th run revealed that the ruthenium nanoparticles remained monodisperse with no significant change in size as the mean diameter of 1.7 ± 0.5 nm is comparable to that of 1.8 ± 0.5 nm for a freshly prepared sample of catalyst **2**.

As the decrease in conversion with reuse could not be attributed to either leaching or aggregation, we next investigated whether the deactivation or passivation could be caused by coordination of the nitrogen donor of the accumulated tetrahydroquinoline to the active surface ruthenium sites, as this could either block access of the substrate and/or modify the reactivity. Thus, an exploratory poisoning study was conducted by pre-treating **2** with four equivalents of 1,2,3,4-tetrahydroquinoline at 65 °C across a range of pre-stirring times to assess the effect of the potential nitrogen donor group on its activity for the dimethylamine borane-mediated reduction of quinoline. Under the optimum conditions identified above, conversions of 92%, 93% and 92% were obtained after pre-stirring the catalyst with 1,2,3,4-tetrahydroquinoline for 0 min, 20 min and 60 min prior to the addition of quinoline. These conversions are similar to that of 94% obtained in the absence of tetrahydroquinoline which suggests that the product that accumulates during each successive run does not passivate or poison the active surface sites. Finally, XPS analysis of the catalyst recovered after five cycles revealed a significant amount of boron fouling on the surface which we believe to be the most likely explanation for the reduction in activity with reuse (see Figure S14–S15 in the supporting information for the corresponding XPS data).

Having identified optimum conditions for the selective reduction of quinoline to 1,2,3,4-tetrahydroquinoline, the protocol was applied to the transfer hydrogenation of a range of substituted quinolines to assess the efficiency and scope of **2** and to evaluate its performance against existing systems. Reactions were first conducted at 65 °C in toluene for 4 h to obtain comparative performance data as a function of the substrate; reaction times were subsequently adjusted accordingly to investigate the influence of reaction time on the conversion and selectivity for either the 1,2-dihydroquinoline or the 1,2,3,4-tetrahydroquinoline, full details of which are presented in Table 2. For each substrate examined, the identity of the products was confirmed by comparison of the NMR spectroscopic data with an authentic sample, in conjunction with the associated mass spectrum. A high conversion was obtained for 6-bromoquinoline which was reduced to a mixture of 6-bromo-1,2-dihydroquinoline as the major species (60%) together with 6-bromo-1,2,3,4-tetrahydroquinoline (40%) after a reaction time of 4 h, with no evidence for competing hydrodehalogenation to quinoline or its reduction products. To
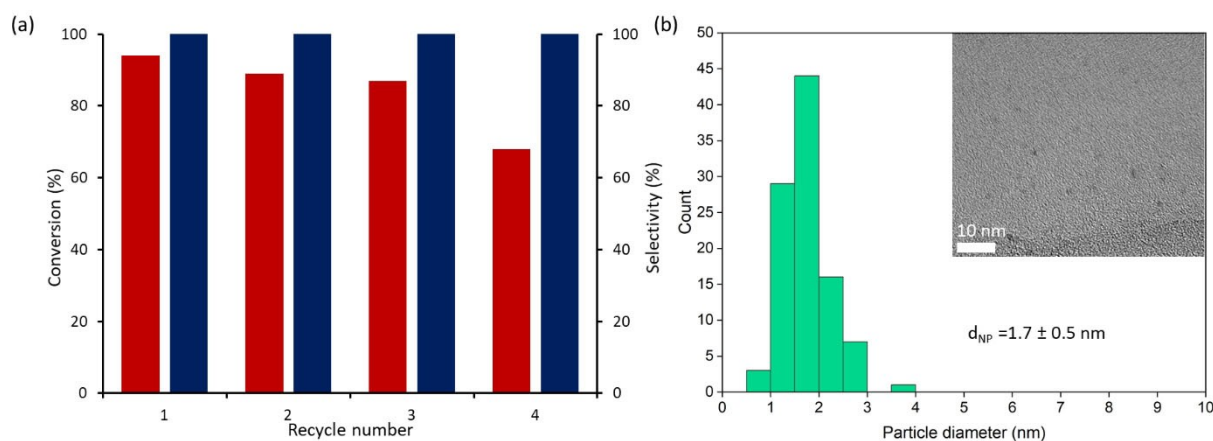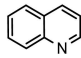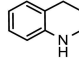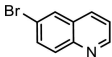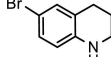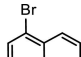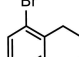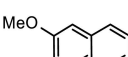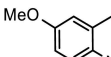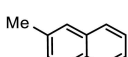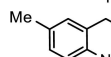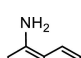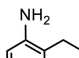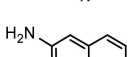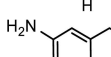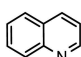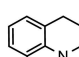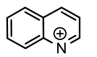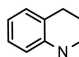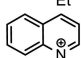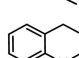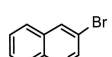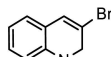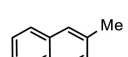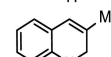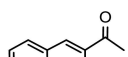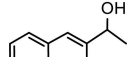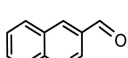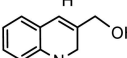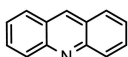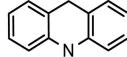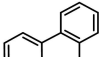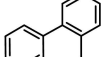

Figure 7. (a) Reuse study for the dimethylamine borane-mediated reduction of quinoline to 1,2,3,4-tetrahydroquinoline conducted in toluene at 65 °C for 4 h catalysed by 0.25 mol% **2**. Red bars – conversion of quinoline, blue bars – selectivity for 1,2,3,4-tetrahydroquinoline and (b) sizing histogram of RuNPs for **2** after four reuses and a TEM image of the recovered material, revealing an average NP diameter of 1.7 ± 0.5 nm, scale bar = 10 nm.

ChemCatChem

Research Article
doi.org/10.1002/cctc.202300418

Chemistry
Europe
European Chemical
Societies Publishing

Table 2. Reduction of quinolines to the corresponding 1,2-dihydroquinoline and 1,2,3,4-tetrahydroquinoline catalysed by 0.25 mol% **2**.[a]

Entry	Substrate	Product	Time [min]	Conv. [%][b,c]	Selectivity [%][c,d]
1			240	96	99
2			240/600	94/93	40/51
3			240/600	91/91	30/40
4			240/1440	39/76	100/100
5			240/960	87/100	78/98
6			240/1440	91/98	54/80
7			240/1440	71/88	68/82
8			1440	12	100
9			240/960	65/99	100/100
10			240/1980	47/100	62/97
11			240	97	100
12			480	94	100
13			240/360	72/100	100/100
14			240/360	80/100	100/100
15			60	100	100
16			60	100	100

[a] Reaction conditions: Conducted under nitrogen, 1.0 mmol substrate, 0.25 mol% **2**, 3 mL toluene, 5.0 mmol dimethylamine borane, 65 °C, time, [b] % Conversion determined by ^{1}H NMR spectroscopy using dioxane as the internal standard. Average of three runs, [c] Reactions were initially run for either 60 min or 240 min to obtain comparative conversion data for each substrate and where required a second reaction was conducted for an appropriate time to reach high conversion; the corresponding reaction times, conversions and selectivities are separated by the / symbol, [d] Selectivity for either 1,2-DHQ or 1,2,3,4-THQ = [% 1,2-DHQ or % 1,2,3,4-THQ/(% 1,2,3,4-tetrahydroquinoline + % 1,2-dihydroquinoline)] × 100 %.

this end, facile hydrodehalogenation of bromo- and chloro-substituted substrates has been reported previously for a range of nanoparticle-based catalysts including metal-carbon stabilised PdNPs,[46] AuNPs deposited on titania,[39] RuNPs supported on biomass-derived N-doped porous carbon nanosheets,[42] AuNPs supported on amine-modified silica,[38] Ni(II)/bis(pyrazolyl)pyridine,[31c] partially reduced Pt/γ-Fe$_2$O$_3$[53a] and PtZn/SiO$_2$.[53b] Thus, the selective reduction of bromo-substituted quinolines without C—Br bond cleavage is a distinct advantage of catalyst **2** for its use in synthesis. Interestingly, an increase in the reaction time to 24 h resulted in only a minor increase in the amount of 6-bromo-1,2,3,4-tetrahydroquinoline to 51%, with a concomitant reduction in the amount of 1,2-dihydroquinoline. A similar conversion and composition-time profile was also obtained for the reduction of 5-bromoquinoline which gave high conversion to a 70:30 mixture of the corresponding dihydroquinoline and tetrahydroquinoline after 4 h; moreover, this ratio did not change significantly even when the reduction was conducted in the presence of ten equivalents of NMe$_2$H.BH$_3$ (Table 2, entries 2–3). Under the same conditions, reduction of the electron rich substrate 6-methoxyquinoline reached 39% conversion after 4 h with 100% selectivity for 6-methoxy-1,2,3,4-tetrahydroquinoline; this conversion improved to 76% to afford 6-methoxy-1,2,3,4-tetrahydroquinoline as the sole product when the reaction time was extended to 24 h. In contrast, 6-methylquinoline reached 87% conversion to afford a mixture of 6-methyl-1,2-dihydroquinoline (22%) and 6-methyl-1,2,3,4-tetrahydroquinoline (78%) after 4 h and 100% conversion with 98% selectivity for 6-methyl-1,2,3,4-tetrahydroquinoline after 16 h (Table 2, entries 4–5). Good conversions were also obtained for the reduction of 5- and 6-aminoquinoline after 4 h, albeit with low selectivity for the corresponding 1,2,3,4-tetrahydroquinoline. However, both the conversion and the selectivity for the corresponding tetrahydroquinoline improved when the reaction time was increased to 24 h (Table 2, entries 6–7). The sterically congested 8-methylquinoline was markedly more challenging and only reached 11% conversion to the 8-methyl-1,2,3,4-tetrahydoquionoline after 24 h at 80 °C (Table 2, entry 8). This substrate is particularly challenging and low conversions have been reported with nanoparticle-based catalysts. The transfer hydrogenation of N-ethyl quinolinium bromide occurred cleanly and gave good conversion to N-ethyl-1,2,3,4-tetrahydroquinoline as the sole product after only 4 h and complete conversion after 16 h (Table 2, entry 9). The corresponding reduction of quinoline N-oxide resulted in deoxygenation and reached complete conversion with 97% selectivity for tetrahydroquinoline after 24 h (Table 2, entry 10). To this end, N-activation of quinolines as their N-oxides has recently been shown to trigger nucleophilic addition of hydrogen and facilitate catalytic transfer hydrogenation using ethanol as a renewable hydrogen source; similarly, pyridines and quinolines have also been activated towards nucleophilic addition by N-alkylation to the corresponding pyridinium bromide; this latter approach successfully prevented undesired re-aromatisation.[54] While dihydroquinolines were identified as intermediates during the hydrogenation of the substituted quinolines investigated in this study, and in some cases were

the major species in the early stages of the reaction, selective partial reduction of quinolines to the corresponding dihydroquinolines is extremely challenging as the product is highly reactive towards further reduction to the tetrahydroquinoline. Remarkably, under the optimum conditions identified above, the reduction of quinolines substituted at the 3-position occurred rapidly and with quantitative conversion to the corresponding 1,2-dihydroquinoline as the sole product. For example, 3-bromo- and 3-methylquinoline were both reduced with 100% selectivity to the corresponding 3-substituted dihydroquinoline (Table 2, entries 11–12). Under the same conditions, the selective partial reduction of 3-acetylquinoline and 3-quinolinecarboxaldehyde was accompanied by reduction of the carbonyl group to afford 1-(1,2-dihydroquinolin-3-yl)ethan-1-ol and (1,2-dihydroquinolin-3-yl)methanol, respectively, as the sole product at complete conversion with no evidence for either tetrahydroquinoline (Table 2, entries 13–14). When the transfer hydrogenation of 3-acetylquinoline and 3-quinolinecarboxaldehyde was conducted at room temperature under otherwise identical conditions, the acyl and aldehyde groups were rapidly and quantitatively reduced to afford 1-(quinolin-3-yl)ethan-1-ol and quinolin-3-ylmethanol, respectively, after only 60 min; selective partial reduction to the corresponding dihydroquinoline was then achieved by adding a further five equivalents of dimethylamine borane and increasing the reaction temperature to 65 °C for 6 h. While it is tempting to attribute this selective partial reduction to the steric influence of the substituent, there are very few reports of the selective reduction of this class of substrate and AuNPs supported on amine functionalised silica,[34,38] nanolayered Co–Mo sulfides,[55] ruthenium nanoclusters supported on Ti$_3$C$_2$T$_x$ nanosheets,[50] PEG-stabilised rhodium nanoparticles,[12] NiNPs in porous carbon[31d] and RuNPs stabilised in silica nanospheres coated with a microporous silica layer, RuSiO$_2$@mSiO$_2$,[33c] all catalyse the reduction of 3-substituted quinolines to afford high yields of the corresponding tetrahydroquinoline with no evidence for the dihydroquinoline, which suggests that the substituent is not the only factor responsible for the high selectivity achieved with **2**. Moreover, reductions conducted in the presence of ten equivalents of dimethylamine borane for extended reaction times also gave the dihydroquinoline as the major species with only a minor amount of the tetrahydroquinoline. The transfer hydrogenation of phenanthridine and acridine also resulted in rapid partial reduction to afford 5,6-dihydrophenanthridine and 9,10-dihydroacridine, respectively, with 100% selectivity at complete conversion (Table 2, entries 15–16). While the partial transfer hydrogenation of quinolines to 1,2-dihydroquinolines has recently been achieved with remarkable selectivity using a homogeneous cobalt(II) phosphinoamido cooperative catalyst and amine borane as the hydrogen donor,[29] this is the first report of the selective partial reduction of 3-substituted quinolines to the corresponding 1,2-dihydroquinolines with a nanoparticle-based catalyst.

In addition to their use as reagents for the synthesis of chiral tetrahydroquinolines, 1,2-dihydroquinolines have been reported to be effective hydrogen transfer reagents. The effectiveness of 3-methyl-1,2-dihydroquinoline as a hydrogen

source was examined by heating a d$_8$-toluene solution of 3-methyl-1,2-dihydroquinoline at 65 °C and monitoring the progress of the reaction as a function of time using ¹H NMR spectroscopy to quantify the composition (see Figure S2 in the supporting information for the corresponding NMR spectra). The resulting profile in Figure 8 shows that the concentration of the 3-methyl-1,2-dihydroquinoline gradually decreases with concomitant formation of 8-methylquinoline as the only spectroscopically observable product i.e. there was no evidence for disproportionation to afford 3-methyl-1,2,3,4-tetrahydroquinoline. This pathway has previously been identified for the formic acid-mediated reduction of 2-methylquinoline using AuNPs supported on amino modified silica. While deuterium labelling experiments identified multiple reaction pathways for the transfer hydrogenation of 2-methylquinoline, 1,2-addition of hydride followed by subsequent disproportionation of the resulting 2-methyl-1,2-dihydroquinoline was established to be the major pathway.[38,56] A similar composition profile was also obtained for 3-bromo-1,2-dihydroquinoline although the release of hydrogen was qualitatively faster than that for 3-methyl-1,2-dihydroquinoline (Figure 8). The liberation of hydrogen was confirmed by conducting a transfer hydrogenation experiment between 3-methyl-1,2-dihydroquinoline and 1,1-diphenylethene in toluene at 60 °C using 5 wt% Pd/C as the catalyst. After 2 h, analysis of the crude reaction mixture by ¹H NMR spectroscopy showed the presence of 1,1-diphenylethane as evidenced by characteristic multiplets at δ 1.67 (d, $J = 7.4$ Hz) and δ 4.19 (q, $J = 7.4$ Hz), which is consistent with transfer hydrogenation (Scheme 2).

Proposed Mechanism for the Reduction of Quinoline

Considering that **2** catalyses the release of hydrogen from dimethylamine borane in water and toluene, the reduction of quinoline could occur either via a heterolytic pathway involving transfer of a hydride and a proton from the hydrogen donor, as

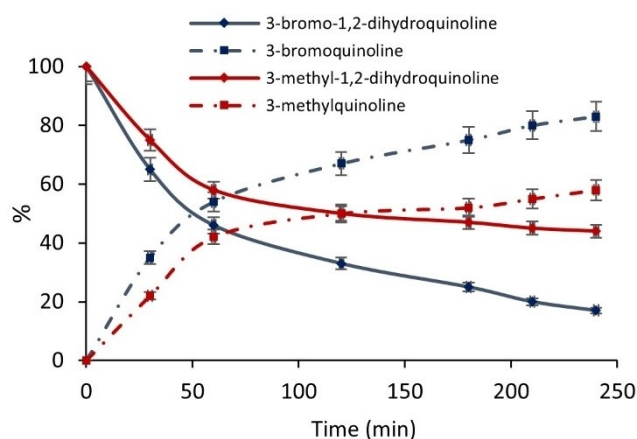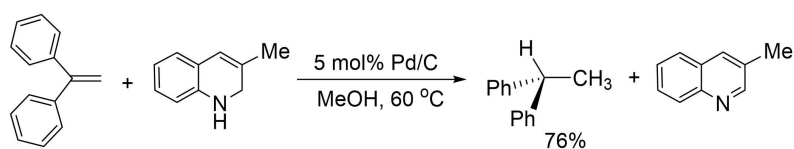**Figure 8.** Composition of d$_8$-toluene solutions of 3-methyl-1,2-dihydroquinoline and 3-bromo-1,2-dihydroquinoline heated at 65 °C as a function of time showing the liberation of hydrogen to form 3-methylquinoline and 3-bromoquinoline, respectively.

Scheme 2. Transfer hydrogenation of 1,1-diphenylethene in methanol using 3-methyl-1,2-dihydroquinoline as the hydrogen donor catalysed by 5 mol% Pd/C.

previously described for the reduction of quinoline with sodium borohydride catalysed by hectorite supported RuNPs[33a] and formic acid/triethylamine catalysed by AuNPs supported on amine-functionalised silica,[38] or *via* homolytic activation of molecular hydrogen liberated *in situ* from the dimethylamine borane. However, as a catalytic hydrogenation of quinoline conducted at 65 °C under 1 atm of hydrogen in the presence of 0.25 mol% **2** only reached 14% conversion after 4 h the reduction probably occurs via a heterolytic pathway involving transfer of a hydride and a proton from the hydrogen donor to the surface of the nanoparticle to afford the active hydride. On this basis, we tentatively suggest that the amino group on the surface of the polymer support may have multiple roles, the first of which is to facilitate heterolytic release of hydrogen from the dimethylamine borane to afford an active surface hydride and an ammonium ion, possibly via a cooperative amine-assisted concerted deprotonation-hydride transfer, as shown in Scheme 3 step (i). However, at this stage we cannot unequivocally exclude the possibility of a direct transfer of the hydride from the amine borane to the C(2) carbon atom of an activated surface coordinated quinoline involving a hydrogen bonded ensemble such as that shown in the insert in Scheme 3. The support grafted primary amine could also form a hydrogen bond with the nitrogen atom of the quinoline which would assist coordination of the substrate via the nitrogen atom rather than the arene ring; such an interaction has been proposed to account for the selective hydrogenation of the N-heterocyclic ring whereas adsorption through the phenyl ring results in its

hydrogenation to afford 5,6,7,8-tetrahydroquinoline (^{5}THQ). In addition, this hydrogen bond would also activate the quinoline ring towards transfer of the hydride to the most electron poor atom of the quinoline (C2) while the ammonium-derived proton would attack the nitrogen atom to generate the dihydroquinoline, as shown in Scheme 3 steps (ii)–(iii); a subsequent hydride addition to C(4) followed by protonation at C(3) would generate the corresponding tetrahydroquinoline. Furthermore, a hydrogen bond between the amino group on the support and the nitrogen atom of the reduced product will also weaken its interaction with the surface ruthenium atom and thereby assist dissociation and prevent poisoning of the catalyst.

While preliminary investigations into the effect of the polymer composition on catalyst performance indicate that the various components of the catalyst influence the conversion as complete selectivity for tetrahydroquinoline is maintained for the dimethylamine borane mediated reduction of quinoline when the PEG and the amino groups are removed, it will be informative to explore whether this design principle can be applied to achieve high selectivity for the hydrogenation of quinolines in aprotic and protic solvents and thereby test the validity of our current understanding. To this end, further catalyst modifications, *in operando* surface investigations and kinetic and computational studies are currently underway to develop a more detailed understanding of the factors that influence catalyst performance and to inform the design of more efficient catalysts.
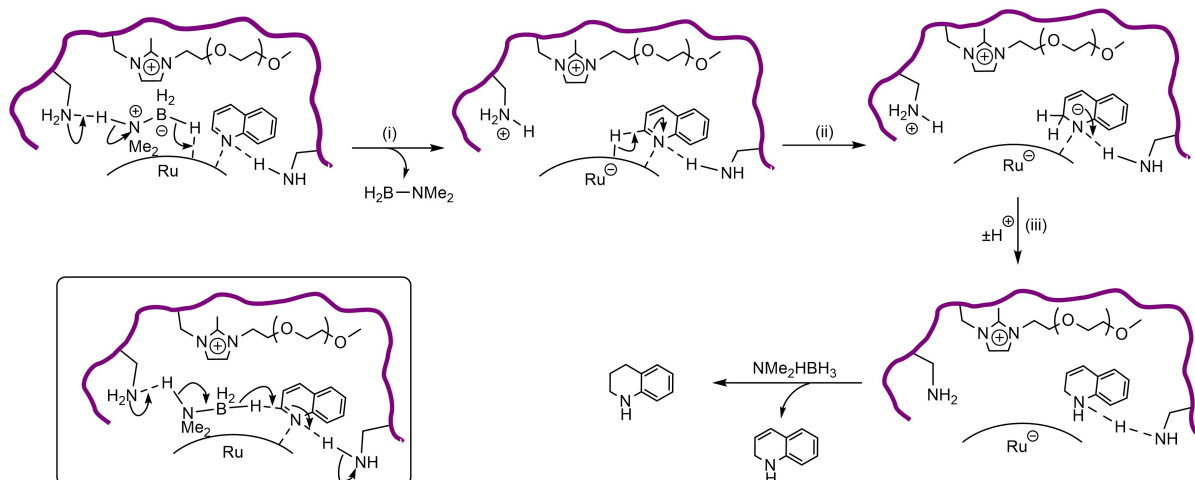
Scheme 3. Possible pathway for the dimethylamine borane-mediated reduction of quinoline involving amine-assisted hydride transfer and hydrogen bond directed coordination and activation of quinoline.

ChemCatChem

Research Article
doi.org/10.1002/cctc.202300418

Chemistry
Europe

European Chemical
Societies Publishing

Conclusions

This study has revealed that ruthenium nanoparticles stabilised by an amine-decorated imidazolium-based polymer immobilised ionic liquid, RuNP@NH$_2$-PEGPIILS, is a remarkably efficient catalyst for the dimethylamine borane-mediated reduction of quinoline to 1,2,3,4-tetrahydroquinoline (THQ) via 1,2-dihydroquinoline. The initial TOF of 610 mol of quinoline converted mol Ru^{-1} h^{-1} for the reduction of quinoline is among the highest to be reported for a metal nanoparticle-based catalyst. Under optimised conditions, a wide range of substituted quinolines were reduced to a mixture of the corresponding 1,2-dihydroquinoline and 1,2,3,4-tetrahydroquinoline in short reaction times and ultimately to the 1,2,3,4-tetrahydroquinoline as the major product by extending the reaction time accordingly. Remarkably, the reduction of 3-substituted quinolines occurred with 100% selectivity for the corresponding partially reduced 1,2-dihydro-quinolines, which were obtained as the sole products in near quantitative yields. Complete selectivity for the partial reduction of 3-substituted quinolines to the corresponding 1,2-dihydroqi-nolines is unprecedented for a nanoparticle-based catalyst and as such this system may well be useful for synthesis involving this class of substrate. In operando surface investigations and kinetic studies are currently underway to develop a more detailed understanding of the selectivity of this system. This is also the first report of a nanoparticle-catalysed hydrogenation of quinoline using dimethylamine borane as the hydrogen donor. The partial reduction of 3-substituted quinolines was shown to be reversible and 8-methyl-1,2-dihydroquinoline acted as an effective hydrogen donor for the palladium-catalysed reduction of 1,1-diphenylethene. Catalyst poisoning studies showed that the NPs were not deactivated by the 1,2,3,4-tetrahydroquinoline product and the gradual decrease in conversion during reuse was most likely due to fouling by the accumulation of boron containing species on the surface of the nanoparticle, as evidence by an XPS study of spent catalyst. Studies are currently underway on polymer modifications to explore which components of this NP-polymer system are required to achieve high activity and porous ionic liquid polymers are being prepared to improve catalyst reusability and longevity.

Experimental

Materials

All reagents were purchased from commercial suppliers and used without further purification, RuCl$_3$.3H$_2$O 99.9% (PGM basis) was purchased form Alfa Aesar (47182) and polymer **1** and catalysts **3–5** were prepared as previously described,[28c,f] and their purity confirmed by ^{1}H and ^{13}C{^{1}H} NMR spectroscopy and elemental analysis. Ethanol was distilled over iodine activated magnesium with a magnesium loading of 5.0 g L^{-1}, diethyl ether from Na/K alloy and toluene from sodium under an atmosphere of nitrogen.

Synthesis of RuNP@NH$_2$-PEGPIILS (2). To a round bottom flask charged with **1** (4.00 g, 5.11 mmol) and ethanol (100 mL) was added a solution of RuCl$_3$·3H$_2$O (1.06 g, 5.11 mmol) in ethanol (20 mL). The resulting mixture was stirred vigorously for 5 hours at room temperature after which time a solution of NaBH$_4$ (1.54 g, 40.9 mmol) in water (10 mL) was added dropwise and the suspension stirred for an additional 18 h before concentrating to dryness under vacuo. The crude black solid was triturated with cold acetone (2×100 mL) then washed with water (100 mL) followed by ethanol (2×50 mL) to afford a black solid that was recovered from the washings via centrifugation followed by filtration through a frit. The final product was rinsed with ether until a fine black powder was obtained which was dried under vacuum to afford **2** in 79% yield (3.45 g). ICP-OES data: ICP-OES data: 6.97 wt% ruthenium and a ruthenium loading of 0.69 mmol g^{-1}.

General Procedure for the Reduction of Quinolines. Under an inert atmosphere, an oven-dried Schlenk flask was charged with **2** (3.6 mg, 0.25 mol%), dimethylamine borane (294 mg, 5.0 mmol) and anhydrous toluene (3 mL). After allowing the resulting suspension to stir for 5 minutes, quinoline (0.118 mL, 1.0 mmol) was added and the mixture stirred at the specified temperature for the allocated time. The reaction mixture was quenched by addition of deionized water (5 mL), the product extracted with ethyl acetate (3×5 mL), the organic fractions collected, and the solvent removed under reduced pressure to obtain the product. The residue was analyzed by ^{1}H NMR spectroscopy using 1,4-dioxane as internal standard to quantify the composition of starting material and products and to determine the selectivity.

Procedure for the Hot Filtration Study. Quinoline (0.118 mL, 1.0 mmol) was reduced to tetrahydroquinoline with dimethylamine borane (294 mg, 5.0 mmol) using 0.1 mol% **2** (1.44 mg) in toluene at 65 °C following the general procedure described above. After 60 minutes the reaction mixture was filtered through a 0.45-micron syringe filter into a clean Schlenk flask under an inert atmosphere. The filtered reaction mixture was then stirred at 65 °C for a further 180 minutes and the progress of the reaction monitored as a function of time by removing aliquots for analysis by NMR spectroscopy.

Procedure for the Catalyst Reuse Study. Quinoline (0.118 mL, 1.0 mmol) was reduced to tetrahydroquinoline with dimethylamine borane (294 mg, 5.0 mmol) at 65 °C in toluene using 0.25 mol% **2** (3.6 mg) following the general procedure described above and the progress of the reaction monitored by removing a small aliquot for analysis by ^{1}H NMR spectroscopy. When the quinoline had been completely consumed the reaction flask was recharged with a further portion of quinoline and a further five equivalents of (CH$_3$)$_2$NH.BH$_3$ (294 mg, 5.0 mmol) and the procedure repeated. Following the 4th run the catalyst was isolated, washed with water (2×10 mL) and ethyl acetate and analysed by TEM.

General Procedure for the Poisoning Studies as a Function of Pre-stirring Time. An oven-dried Schlenk flask cooled to room temperature under vacuum, back-filled with nitrogen and charged with **2** (3.6 mg, 0.25 mol%), dimethylamine borane (294 mg, 5.0 mmol), anhydrous toluene (3 mL) and 1,2,3,4-tetrahydroquino-line (1.0 mmol) and the resulting mixture was stirred for the allocated time (0, 20, or 60 min) to explore the effect of pre-stirring time on catalyst efficacy. Reaction was initiated by the addition of quinoline (0.118 mL, 1.0 mmol) and the mixture was left to stir for 4 h at room temperature. The reaction mixture was quenched by addition of deionized water (5 mL), the product extracted with ethyl acetate (3×5 mL), the organic fractions collected, and the solvent removed under reduced pressure. The resulting residue was analyzed by ^{1}H NMR spectroscopy to quantify the composition of starting material and products and to determine the selectivity.

ChemCatChem

Research Article
doi.org/10.1002/cctc.202300418

**Chemistry
Europe**
European Chemical
Societies Publishing

Acknowledgements

Conflict of Interests

The authors declare that they have no known competing financial interests or personal relationships that could have appeared to influence the work reported in this paper.

Data Availability Statement

The data that support the findings of this study are available in the supplementary material of this article.

[1] a) M. El-Shahat, *J. Heterocycl. Chem.* **2022**, *59*, 399–421; b) I. Muthukrishnan, V. Sridharan, J. C. Menendez, *Chem. Rev.* **2019**,*119*, 5057–5191; c) V. Sridharan, P. A. Suryavanshi, J. C. Menéndez, *Chem. Rev.* **2011**, *111*, 7157–7259; d) R. P. Filho, C. M. Souza Menezes, P. L. S. Pinto, G. A. Paula, C. A. Brandt, M. A. B. Silveira, *Bioorg. Med. Chem.* **2007**, *15*, 1229–1236; e) J. D. Scott, R. M. Williams, *Chem. Rev.* **2002**, *102*, 1669–1730; f) C. Deraedt, R. Ye, W. T. Ralston, F. D. Toste, G. A. Somorjai, *J. Am. Chem. Soc.* **2017**, *139*, 18084–18092.

[2] a) C. Wang, C. Li, X. Wu, A. Pettman, J. Xiao, *Angew. Chem. Int. Ed.* **2009**, *48*, 6524–6528; *Angew. Chem.* **2009**, *121*, 6646–6650; b) G. E. Dobereiner, A. Nova, N. D. Schley, N. Hazari, S. J. Miller, R. H. Crabtree, *J. Am. Chem. Soc.* **2011**, *133*, 7547–7562; c) D. Zhao, L. Candish, D. Paul, F. Glorius, *ACS Catal.* **2016**, *6*, 5978–5988; d) Y. Alvarado, M. Busolo, F. López-Linares, *J. Mol. Cat. A Chem.* **1999**, *142*, 163–167; e) R. Kuwano, R. Ikeda, K. Hirasada, *Chem. Commun.* **2015**, *51*, 7558–7561; f) M. P. Wiesenfeldt, Z. Nairoukh, T. Dalton, F. Glorius, *Angew. Chem. Int. Ed.* **2019**, *58*, 10460–10476; *Angew. Chem.* **2019**, *131*, 10570–10586; g) Á. Vivancos, M. Beller, M. Albrecht, *ACS Catal.* **2018**, *8*, 17–21; h) H. Zhou, Z. Li, Z. Wang, T. Wang, L. Xu, Y. He, Q.-H. Fan, J. Pan, L. Gu, A. S. C. Chan, *Angew. Chem. Int. Ed.* **2008**, *47*, 8464–8467; *Angew. Chem.* **2008**, *120*, 8592–8595; i) Z. Yang, F. Chen, Y.-M. He, N. Yang, Q.-H. Fan, *Catal. Sci. Technol.* **2014**, *4*, 2887–2890; j) P. Sánchez, M. Hernández-Juárez, N.

Rendón, J. López-Serrano, L. L. Santos, E. Álvarez, M. Paneque, A. Suárez, *Dalton Trans.* **2020**, *49*, 9583–9587.

[3] a) L. Bai, X. Wang, Q. Chen, Y. Ye, H. Zheng, J. Guo, Y. Yin, C. Gao, *Angew. Chem. Int. Ed.* **2016**, *55*, 15656–15661; *Angew. Chem.* **2016**, *128*, 15885–15890; b) R. A. Van Santen, *Acc. Chem. Res.* **2009**, *42*, 57–66; c) S. Vajda, M. J. Pellin, J. P. Greeley, C. L. Marshall, L. A. Curtiss, G. A. Ballentine, J. W. Elam, S. Catillon-Mucherie, P. C. Redfern, F. Mehmood, P. Zapol, *Nat. Mater.* **2009**, *8*, 213–216; d) R. Jin, C. Zeng, M. Zhou, Y. Chen, *Chem. Rev.* **2016**, *116*, 10346–10413.

[4] Y.-P. Sun, H.-Y. Fu, D.-l. Zhang, R.-X. Li, H. Chen, X.-J. Li, *Catal. Commun.* **2010**, *12*, 188–192.

[5] H. Konnerth, M. H. G. Prechtl, *Green Chem.* **2017**, *19*, 2762–2767.

[6] a) M. M. Dell'Anna, V. F. Capodiferro, M. Mali, D. Manno, P. Cotugno, A. Monopoli, P. Mastrorilli, *Appl. Catal. A General* **2014**, *48*, 89–95; b) M. M. Dell'Annaa, G. Romanazzi, S. Intini, A. Rizzuti, C. Leonelli, A. F. Piccinni, P. Mastrorilli, *J. Mol. Catal. A:* **2015**, *402*, 83–91.

[7] S. Zhang, Z. Xia, T. Ni, Z. Zhang, Y. Ma, Y. Qu, *J. Catal.* **2018**, *359*, 101–111.

[8] X. Yu, R. Nie, H. Zhang, X. Lu, D. Zhou, Q. Xia, *Microporous Mesoporous Mater.* **2018**, *256*, 10–17.

[9] N. A. Beckers, S. Huynh, X. Zhang, E. J. Luber, J. M. Buriak, *ACS Catal.* **2012**, *2*, 1524–1534.

[10] J. Zhao, H. Yuan, X. Qin, K. Tian, Y. Liu, C. Wei, Z. Zhang, L. Zhou, S. Fang, *Catal. Lett.* **2020**, *150*, 2841–2849.

[11] D. Ren, L. He, L. Yu, R.-S. Ding, Y.-M. Liu, Y. Cao, H.-Y. He, K.-N. Fan, *J. Am. Chem. Soc.* **2012**, *134*, 17592–17598.

[12] M. Niu, Y. Wang, P. Chen, D. Du, J. Jiang, Z. Jin, *Catal. Sci. Technol.* **2015**, *5*, 4746–4749.

[13] X. Wang, W. Chen, L. Zhang, T. Yao, W. Liu, Y. Lin, H. Ju, J. Dong, L. Zheng, W. Yan, X. Zheng, Z. Li, X. Wang, J. Yang, D. He, Y. Wang, Z. Deng, Y. Wu, Y. Li, *J. Am. Chem. Soc.* **2017**, *139*, 9419–9422.

[14] T.-N. Ye, J. Li, M. Kitano, H. Hosono, *Green Chem.* **2017**, *19*, 749–756.

[15] X. Xue, M. Zeng, Y. Wang, *Appl. Catal. A General* **2018**, *560*, 37–41.

[16] F. Chen, A.-E. Surkus, L. He, M.-M. Pohl, J. Radnik, C. Topf, K. Junge, M. Beller, *J. Am. Chem. Soc.* **2015**, *137*, 11718–11724.

[17] J. Zhao, H. Yuan, G. Yang, Y. Liu, X. Qin, Z. Chen, C. Weng-Chon, L. Zhou, S. Fang, *Nano Res.* **2022**, *15*, 1796–1802.

[18] B. Sahoo, C. Kreyenschulte, G. Agostini, H. Lund, S. Bachmann, M. Scalone, K. Junge, M. Beller, *Chem. Sci.* **2018**, *9*, 8134–8141.

[19] Z. Wei, Y. Chen, J. Wang, D. Su, M. Tang, S. Mao, Y. Wang, *ACS Catal.* **2016**, *6*, 5816–5822.

[20] a) D.-S. Wang, Q.-A. Chen, S.-M. Lu, Y.-G. Zhou, *Chem. Rev.* **2012**, *112*, 2557–2590; b) Y.-G. Zhou, *Acc. Chem. Res.* **2007**, *40*, 1357–1366.

[21] a) For a comprehensive and highly informative review on the impact of ligands on heterogeneous nanocatalysis see L. Lu, Z. Zou, B. Fang, *ACS Catal.* **2021**, *11*, 6020–6058; b) K. Liu, R. Qin, N. Zheng, *J. Am. Chem. Soc.* **2021**, *143*, 4483–4499; c) For an insightful account on metal nanoparticles immobilised on molecularly modified surfaces for controlled hydrogenation and hydrogenolysis see A. Bordet, W. Leitner, *Acc. Chem. Res.* **2021**, *54*, 2144–2157; d) L. M. Rossi, J. L. Fiorio, M. A. S. Garcia, C. P. Ferraz, *Dalton Trans.* **2018**, *47*, 5889–5915; e) S. Campisi, M. Schiavoni, C. E. Chan-Thaw, A. Villa, *Catalysts* **2016**, *6*, 185; f) X. Wang, Y.-F. Jiang, Y.-N. Liu, A.-W. Xu, *New J. Chem.* **2018**, 19901–19907; g) M. Sankar, Q. He, R. V. Engel, M. A. Sainna, A. J. Logsdail, A. Roldan, D. J. Willock, N. Agarwal, C. J. Kiely, G. J. Hutchings, *Chem. Rev.* **2020**, *120*, 3890–3938; h) C. Wu, D. Cheng, M. Wang, D. Ma, *Energy Fuels* **2021**, *35*, 19012–19023; i) T. Pu, W. Zhang, M. Zhu, *Angew. Chem. Int. Ed.* **2023**, *62*, e202212278; j) C. Gao, F. Lyu, Y. Tin, *Chem. Rev.* **2021**, *121*, 834–881; k) T. W. van Deelen, C. H. Mejía, K. P. de Jong, *Nature Catalysis* **2019**, *2*, 955–970; l) Z. Luo, G. Zhao, H. Pan, W. Sun, *Adv. Energy Mater.* **2022**, *12*, 2201395.

[22] a) H. Liu, Q. Mei, S. Li, Y. Yang, Y.-Y. Wang, H. Liu, L.-R. Zheng, P. An, J. Zhang, B. Han, *Chem. Commun.* **2018**, *54*, 908–911; b) S. Rana, S. B. Jonnalagadda, *RSC Adv.* **2017**, *7*, 4869–2879; c) Z. Guo, C. Xiao, R. V. Maligal-Ganesh, L. Zhou, T. W. Goh, X. Li, D. Tesfagaber, A. Thiel, W. Huang, *ACS Catal.* **2014**, *4*, 1340–1348; d) Z. Tian, D.-L. Chen, T. He, P. Yang, F.-F. Wang, Y. Zhong, W. Zhu, *Phys. Chem. Chem. Phys.* **2019**, *123*, 22114–22122; e) B. Wu, B. Huang, J. Yang, N. Zheng, G. Fu, *Angew. Chem. Int. Ed.* **2012**, *51*, 3440–3443; *Angew. Chem.* **2012**, *124*, 3496–3499.

[23] a) M. Guo, C. Li, Q. Yang, *Catal. Sci. Technol.* **2017**, *7*, 2221–2227; b) D Chandra, S. Saini, S. Bhattacharya, A. Bhaumik, K. Kamata, M. Hara, *ACS Appl. Mater. Interfaces* **2020**, *12*, 52668–52677; c) X. Cuil, A.-E. Surkus, K. Junge, C. Topf, J. Radnik, C. Kreyenschulte, M. Beller, *Nat. Commun.* **2016**, *7*, 11326.

[24] a) S. G. Kwon, G. Krylova, A. Sumer, M. M. Schwartz, E. E. Bunel, C. L. Marshall, S. Chattopadhyay, B. Lee, J. Jellinek, E. V. Shevchenko, *Nano Lett.* **2012**, *12*, 5382–5388; b) W. Long, N. A. Brunelli, S. A. Didas, E. W. Ping, C. W. Jones, *ACS Catal.* **2013**, *3*, 1700–1708; c) F. P. da Silva, J. L. Fiorio, L. M. Rossi, *ACS Omega* **2017**, *2*, 6014–6022.

[25] a) G. Chen, C. Xu, X. Huang, J. Ye, L. Gu, G. Li, Z. Tang, B. Wu, H. Yang, Z. Zhao, Z. Zhou, G. Fu, N. Zheng, *Nat. Mater.* **2016**, *15*, 564–569; b) E. H. Boymans, P. T. Witte, D. Vogt, *Catal. Sci. Technol.* **2015**, *5*, 176–183; c) M. R. Axet, S. Conejero, I. C. Gerber, *ACS Appl. Nano Mater.* **2018**, *1*, 5885–5894.

[26] a) S. Masuda, K. Mori, Y. Futamura, H. Yamashita, *ACS Catal.* **2018**, *8*, 2277–2285; b) K. Mori, S. Masuda, H. Tanaka, K. Yoshizawa, M. Chee, H. Yamashita, *Chem. Commun.* **2017**, *53*, 4677–4690; c) H. Zhong, M. Iguchi, M. Chatterjee, T. Ishizaka, M. Kitta, Q. Xu, H. Kawanami, *ACS Catal.* **2018**, *8*, 5355–5362; d) V. Srivastava, *Catal. Lett.* **2021**, *151*, 3704–3720; e) Q. Liu, X. Yang, L. Li, S. Miao, Y. Li, Y. Li, X. Wang, Y. Huang, T. Zhang, *Nat. Commun.* **2017**, *8*, 1407.

[27] a) K. Koh, J.-E. Seo, J. H. Lee, A. Goswami, C. W. Yoon, T. Asefa, *J. Mater. Chem. A* **2014**, *2*, 20444–20449; b) K. Koh, M. Jeon, C. Won Yoon, T. Asefa, *J. Mater. Chem. A* **2017**, *5*, 16150–16161; c) Y. Luo, Q. Yang, W. Nie, Q. Yao, Z. Zhang, Z.-H. Lu, *ACS Appl. Mater. Interfaces* **2020**, *12*, 8082–8090; d) M. Yurderi, A. Bulut, N. Caner, M. Celebi, M. Kayab, M. Zahmakiran, *Chem. Commun.* **2015**, *51*, 11417–11420; e) L. Xu, F. Yao, J. Luo, C. Wan, M. Ye, P. Cui, Y. An, *RSC Adv.* **2017**, *7*, 4746–4752; f) Z. Zhang, D. He, Z. Wang, S. Wu, T. Liu, *J. Catal.* **2022**, *410*, 121–127; g) Q. Zhang, Z. Zhu, X. Zhang, P. Li, Y. Huang, X. Luo, Z. Liang, *Int. J. Hydrogen Energy* **2019**, *44*, 16707–16717; h) S.-J. Li, Y.-T. Zhou, X. Kang, D.-X Liu, L. Gu, Q.-H. Zhang, J.-M. Yan, Q. Jiang, *Adv. Mater.* **2019**, *5*, 1806781; i) F.-Z. Song, Q.-L. Zhu, N. Tsumori, Q. Xu, *ACS Catal.* **2015**, *5*, 5141–5144; j) Y.-X. Luo, W. Nie, Y. Ding, Q. Yao, G. Feng, Z.-H. Lu, *ACS Appl. Energ. Mater.* **2021**, *4*, 4945–4954; k) Z. Duan, W. Wu, Q. Lei, H. Chen, *Int. J. Hydrogen Energy* **2022**, *47*, 32050–32059; l) L. Li, X. Chen, C. Zhang, G. Zhang, Z. Liu, *ACS Omega* **2022**, *7*, 14944–14951.

[28] a) S. Doherty, J. G. Knight, T. Backhouse, E. Abood, H. Alshaikh, I. A. J. Fairlamb, R. A. Bourne, T. W. Chamberlain, R. Stones, *Green Chem.* **2017**, *19*, 1635–1641; b) S. Doherty, J. G. Knight, T. Backhouse, A. Bradford, F. Saunders, R. A. Bourne, T. W. Chamberlain, R. Stones, A. Clayton, K. J. R. Lovelock, *Catal. Sci. Technol.* **2018**, *8*, 1454–1467; c) S. Doherty, J. G. Knight, T. Backhouse, E. Abood, H. Alshaikh, A. Clemmet, J. R. Ellison, R. A. Bourne, T. W. Chamberlain, R. Stones, I. A. J. Fairlamb, K. J. R. Lovelock, *Adv. Synth. Catal.* **2018**, *360*, 3716–3731; d) S. Doherty, J. G. Knight, T. Backhouse, T. S. T. Tran, F. Stahl, H. Y. Alharbi, T. W. Chamberlain, R. A. Bourne, R. Stones, J. P. White, Z. Aslam, C. Hardacre, H. Daly, J. Hart, R. H. Temperton, J. N. O'Shea, N. H. Rees, *Catal. Sci. Technol.* **2022**, *12*, 3549–3567; e) S. Doherty, J. G. Knight, H. Y. Alharbi, R. Paterson, C. Wills, C. Dixon, L. Šiller, T. W. Chamberlain, A. Griffiths, S. M. Collins, K–J. Wu, M. D. Simmons, R. A. Bourne, K. R. J. Seymour, *ChemCatChem* **2022**, e202101752; f) S. Doherty, J. G. Knight, R. Paterson, A. A. Alharbi, C. Wills, C. Dixon, L. Šiller, T. W. Chamberlain, A. Griffiths, S. M. Collins, K–J. Wu, M. D. Simmons, R. A. Bourne, K. R. J. Lovelock and J. Seymour, *J. Mol. Catal.* **2022**, *528*, 112476; g) S. Doherty, J. G. Knight, T. Backhouse, W. Simpson, W. Paget, E. Abood, R. A. Bourne, T. W. Chamberlain, R. Stones, K. J. R. Lovelock, J. M. Seymour, M. A. Isaacs, H. Daley, C. Hardacre, N. H. Rees, *ACS Catal.* **2019**, *9*, 4777–4791; h) S. Doherty, J. G. Knight, R. Paterson, C. Wills, T. W. Chamberlain, A. Griffiths, S. M. Collins, K–J. Wu, M. D. Simmons, *J. Catal.* **2023**, *417*, 74–86.

[29] M. Pang, J.-Y. Chn, S. Zhang, R.-Z. Liao, C.-H. Tung, W. Wang, *Nat. Commun.* **2020**, *11*, 1249.

[30] R. Pothikumar, V. T. Bhat, K. Namitharan, *Chem. Commun.* **2020**, *56*, 13607–13610.

[31] a) For a comprehensive and informative review on the use of amine–boranes as transfer hydrogenation and hydrogenation reagents see: S. Lau, D. Gasperini, R. L. Webster, *Angew. Chem. Int. Ed.* **2021**, *60*, 14272–14294; *Angew. Chem.* **2021**, *133*, 14393–14415; b) P. Lara, K. Philippot, A. Suárez, *ChemCatChem* **2019**, *11*, 766–771; c) V. Vermaak, H. C. M. Vosloo, A. J. Swarts, *Adv. Synth. Catal.* **2020**, *362*, 5788–5793; d) R. Yun, W. Ma, L.

Hong, Y. Hu, F. Zhan, S. Liu, B. Zheng, *Catal. Sci. Technol.* **2019**, *9*, 6669–6672; e) C. Gao, Q. Xuan, Q. Song, *Chin. J. Chem.* **2021**, *39*, 2504–2508; f) Y.-F. Zeng, Y.-N. Li, M.-X. Zhou, S. Han, Y. Guo, Z. Wang, *Adv. Synth. Catal.* **2022**, *364*, 3664–3669.

[32] D. J. Morgan, *Surf. Interface Anal.* **2015**, *47*, 1072–1079.

[33] a) B. Sun, D. Carnevale, G. Süss-Fink, *J. Organomet. Chem.* **2016**, *821*, 197–205; b) H.-Y. Jiang, X.-X. Zheng, *Appl. Catal. A General* **2015**, *499*, 118–123; c) L. Zhang, X. Wang, Y. Xue, X. Zeng, H. Chen, R. Li, S. Wang, *Catal. Sci. Technol.* **2014**, *4*, 1939–1948.

[34] a) M. Fang, R. A. Sánchez-Delgado, *J. Catal.* **2014**, *311*, 357–368; b) F. Martinez-Espinar, P. Blondeau, P. Nolise, B. Chaudret, C. Claver, S. Castillón, C. Godard, *J. Catal.* **2017**, *354*, 113–127.

[35] D. E. Minter, C. R. Kelly, H. C. Kelly, *Inorg. Chem.* **1986**, *25*, 3291–3294.

[36] M. Yadav, T. Akita, N. Tsumori, Q. Xu, *J. Mater. Chem.* **2012**, *22*, 12582–12586.

[37] M. N. Shaikh, A. N. Kalanthoden, M. Ali, Md. A. Haque, Md. A. Aziz, M. M. Abdelnaby, S. K. Rani, A. I. Bakare, *ChemistrySelect* **2020**, *5*, 14827–14838.

[38] B. Vilhanová, J. A. van Bokhoven, M. Ranocchiari, *Adv. Synth. Catal.* **2017**, *359*, 677–686.

[39] L. Tao, Q. Zhang, S.-S. Li, X. Liu, Y.-M. Liu, Y. Cao, *Adv. Synth. Catal.* **2015**, *357*, 753–760.

[40] M. Tang, J. Deng, M. Li, X. Li, H. Li, Z. Chen, Y. Wang, *Green Chem.* **2016**, *18*, 6082–6090.

[41] H.-Y. Jiang, X.-X. Zheng, *Catal. Sci. Technol.* **2015**, *5*, 3728–3734.

[42] Y. Cao, L. Ding, Z. Qiu, H. Zhang, *Catal. Commun.* **2020**, *143*, 106048.

[43] H.-y. Jiang, S.-s. Zhang, B. Sun, *Catal. Lett.* **2018**, *148*, 1336–1344.

[44] H. Zhang, A. Peia, J. Liao, L. Ruan, K. Yang, J. Wang, L. Zhu, B. H. Chen, *J. Alloys Compd.* **2020**, *834*, 155203.

[45] Q. Song, D. Xu, W. D. Wang, J. Fang, X. Sun, F. Li, B. Li, J. Kou, H. Zhu, Z. Dong, *J. Catal.* **2022**, *406*, 19–27.

[46] Y. Zhang, J. Zhu, Y.-T. Xia, X.-T. Sun, L. Wu, *Adv. Synth. Catal.* **2016**, *358*, 3039–3045.

[47] S. Rengshausen, C. Van Stappen, N. Levin, S. Tricard, K. L. Luska, S. DeBeer, B. Chaudret, A. Bordet, W. Leitner, *Small* **2021**, *17*, 2006683.

[48] A. Karakulina, A. Gopakumar, İ. Akçok, B. L. Roulier, T. LaGrange, S. A. Katsyuba, S. Das, P. J. Dyson, *Angew. Chem. Int. Ed.* **2016**, *55*, 292–296; *Angew. Chem.* **2016**, *128*, 300–304.

[49] C. Chaudhari, K. Sato, Y. Nishida, T. Yamamoto, T. Toriyama, S. Matsumurac, Y. Ikeda, K. Terada, N. Abe, K. Kusuda, H. Kitagawa, K. Nagaoka, *RSC Adv.* **2020**, *10*, 44191–44195.

[50] X. Zhao, G. Zhang, J. Wang, T. Yuan, J. Huang, L. Wang, Y.-N. Liu, *Appl. Nano Mater.* **2022**, *5*, 6213–6220.

[51] J. Niea, Z. Zhu, Y. Liao, X. Xiao, F. Mauriello, Z. Zhang, *J. Mol. Catal.* **2022**, *526*, 112381.

[52] X. Wang, W. Chen, L. Zhang, T. Yao, W. Liu, Y. Lin, H. Ju, J. Dong, L. Zheng, W. Yan, X. Zheng, Z. Li, X. Wang, J. Yang, D. He, Y. Wang, Z. Deng, Y. Wu, Y. Li, *J. Am. Chem. Soc.* **2017**, *139*, 9419–9422.

[53] a) M. Liang, X. Wang, H. Liu, H. Liu, Y. Wan, *J. Catal.* **2008**, *255*, 335–342; b) S. Iihama, S. Furukawa, T. Komatsu, *ACS Catal.* **2016**, *6*, 742–746.

[54] S. Yadav, D. Chaudhary, N. K. Maurya, D. Kumar, K. Ishua, M. R. Kuram, *Chem. Commun.* **2022**, *58*, 4255–4258.

[55] I. Sorribes, L. Liu, A. Domenech-Carbo, A. Corma, *ACS Catal.* **2018**, *8*, 4545–4557.

[56] a) D. Talwar, H. Y. Li, E. Durham, J. Xiao, *Chem. Eur. J.* **2015**, *21*, 5370–5379; b) T. Wang, L.-G. Zhuo, Z. Li, F. Chen, Z. Ding, Y. He, Q.-H. Fan, J. Xiang, Z.-X. Yu, A. S. C. Chan, *J. Am. Chem. Soc.* **2011**, *133*, 9878–9891; c) T. P. Forrest, G. A. Dauphinee, S. A. Deraniyagala, *Can. J. Chem.* **1985**, *63*, 412–417.